MULTI-HAZARD SUSCEPTIBILITY ASSESSMENT WITH HYBRID MACHINE LEARNING METHODS FOR TUT REGION (ADIYAMAN, TURKIYE)

G. Karakas [1,2], S. Kocaman [2]*, C. Gokceoglu[3]

[1]Graduate School of Science and Engineering, Hacettepe University, 06800 Beytepe, Ankara, Türkiye - gizem.karakas@hacettepe.edu.tr
[2] Dept. of Geomatics Engineering, Hacettepe University, 06800 Beytepe Ankara, Türkiye - sultankocaman@hacettepe.edu.tr
[3] Dept. of Geological Engineering, Hacettepe University, 06800 Beytepe Ankara, Türkiye - cgokce@hacettepe.edu.tr

KEY WORDS: Landslides, Earthquakes, Floods, Random Forest, Fuzzy Inference System, Multi-hazard Susceptibility, Site Selection

ABSTRACT:

Recent Kahramanmaras earthquakes (Mw 7.7 and 7.6) occurred on 6 February 2023 have shown the importance of site selection for settlements and infrastructure considering the fact that multiple hazards may affect the same area and even interact with each other. The Kahramanmaras earthquakes triggered several landslides, which also increased the level of destruction. Here, we implemented a multi-hazard susceptibility assessment approach for Tut town of Golbasi, Adiyaman and its surroundings. Over 600 landslides were triggered in the area by the earthquakes. In addition, the region is prone to flooding and a devastating one occurred on March 15, 2023 after heavy rains. In this study, we employed co-seismic landslide inventory for landslide susceptibility assessment with random forest. Regarding flood susceptibility, a modified analytical hierarchical process was utilized based on expert opinion on factor importance. The earthquake hazard probability distribution was obtained from a distance-based interpolation of Arias intensity values. We utilized Mamdani Fuzzy Inference System for producing a multi-hazard susceptibility map from univariate maps of earthquake, landslide and flood. The result shows that the selected methods for each type of susceptibility map was suitable and the output of the study can be utilized for the site selection in Tut region, which is a crucial subject due to the need of new construction sites after the earthquakes.

1. INTRODUCTION

Hazards can be called natural events that negatively affect life on earth, cause loss of lives and property with their economic, environmental, and physical effects, and pause vital activities. A significant increase was observed in the occurrences of natural hazards in Türkiye and in the world recently. Climate change and urban development, in other words, rapid population growth, in areas highly prone to natural hazards are among the most important reasons for this increase. Due to its geological, geomorphological structure and climatic characteristics, Türkiye frequently encounters natural hazards that cause great loss of life and property. Earthquakes, landslides and floods can be listed among the natural hazards.

Most susceptibility assessment studies in the literature for Türkiye have focused on exclusively on one hazard, although multiple hazards often affect most regions (Karakas et al., 2020, 2023; Tiryaki and Karaca, 2018). In fact, these hazards mostly interact with each other. For this reason, it is necessary to evaluate multiple natural hazards together and to analyze the interactions between them or the effects that trigger each other (Karakas et al., 2023; Yanar et al., 2020). Pourghasemi et al. (2020) conducted a study on multi-hazard probability assessment in the Fars Province for four watersheds. The most important effective factors were selected for flood, forest fire and landslide natural hazards, and then susceptibility maps were predicted with the random forest (RF) algorithm. In order to multi-hazard susceptibility map, all three susceptibility maps were combined by addition.

Rahmati et al. (2019) aimed to produce a multi-hazard exposure map for avalanche, rockfall, and flood hazards in the Asara watershed, Iran. Avalanche, rockfall and flood hazard models were produced with support vector machine (SVM), boosted regression tree (BRT), and generalized additive model (GAM). A multi-hazard map was obtained with the weighted integration method by using the best of the three methods for each hazard model. In addition, in the study, a multi-hazard exposure map was produced by using exposure-related factors such as main road, rural road, residential area, and power transmission line.

Another study by Rusk et al. (2022) proposed a multi-hazard susceptibility assessment and exposure model for floods, landslides, and wildfires. Individual susceptibility maps produced by the maximum entropy (Maxent) method were combined by overlapping and a multi-hazard susceptibility map was produced. Population distribution data was used to determine the exposure. Multi-hazard susceptible areas were the southern and northern parts of the study area.

Karakas et al. (2023) assessed the multi-hazard susceptibility for a part of Elazig Province, Türkiye, considering floods, earthquakes, and landslides. Although the availability of a landslide inventory enabled the use of a data-driven machine learning method, the RF, for susceptibility assessment; an expert-based method, modified analytical hierarchical process (M-AHP), was preferred for flood susceptibility assessment due to the lack of flood inventory. On the other hand, Arias intensity values were utilized for assessing the earthquake hazard. Regarding the multi-hazard susceptibility assessment, again an expert-based approach, the Mamdani Fuzzy Inference System (FIS) was preferred. The membership functions were designed considering the destructive effect of the individual hazard types in the history of the region.

* Corresponding author

On February 6, 2023, two destructive earthquakes occured with magnitudes of Mw. 7.7 and Mw. 7.6 and their epicenters located in Pazarcik and Elbistan districts of Kahramanmaras. The earthquakes caused devastating destructions in 11 provinces in the Eastern and Southeastern Anatolia Region of Turkey. It can be considered as the most disastrous event occurred in Türkiye in the last century, caused damages immeasurable in size, and fatalities in the orders of tens of thousands. Besides devastating earthquakes, the region experienced a large number of secondary hazard events, such as landslide, rockfall, rock avalanche, liquefaction, surface rupture etc. triggered by the earthquakes. In addition, a climate-related meteorological hazard, flooding, is frequently observed in some parts of the region, which may trigger landslides as well. Considering the enormity of damaged settlements, site selection for new construction sites has become more important than ever. Therefore, accurate determination and updating of areas susceptible to natural hazards is of great importance for planning and site selection, and disaster mitigation efforts.

The main aim of this study was to assess multi-hazard probability of a region covering Tut town of Adiyaman province and its surroundings by combining expert-based and supervised machine-learning methods considering landslide, flood and earthquake hazards. Tut town was affected by earthquakes, landslides and flooding (Gaziantep Time, 2023; TRT Haber, 2023) after the Kahramanmaras earthquakes. The proposed multi-hazard assessment approach was previously developed for another region, Elazig (Türkiye) (see Karakas et al., 2023), and the predictive variables and the model parameters were adapted here for the Tut site.

2. MATERIAL AND METHODS

In the following, the study area location, geological characteristics and landslide inventory preparation, geospatial datasets used for the susceptibility mapping, production methods of univariate and multi-hazard susceptibility maps are explained in detail.

2.1. Study Area

Tut town of Adiyaman province and its surroundings in Türkiye was selected as study area. The size of the area is approximately 1590 km^2. Figure 1 shows the location of the study area and the digital elevation model (DEM) obtained from EUDEM v1.1. After the devastating Kahramanmaras earthquakes of February 6, 2023, this region is among the places that were severely affected with heavy damages. Many landslides, which are secondary hazards, were triggered by the effect of the earthquakes. In addition, on March 15, 2023, a flood event occurred in the region due to heavy rain. This flood event caused damage to houses and loss of life. Examples of these natural hazard events are illustrated in Figure 2.

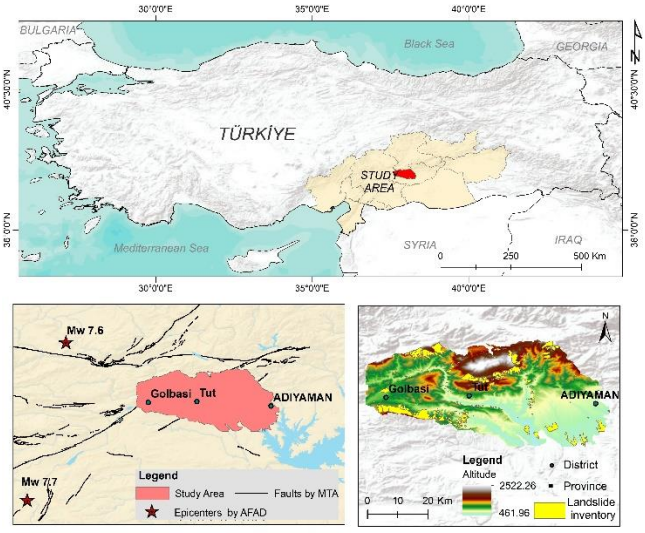

Figure 1. Study area location and the DEM source from EUDEM v1.1 with landslide inventory.

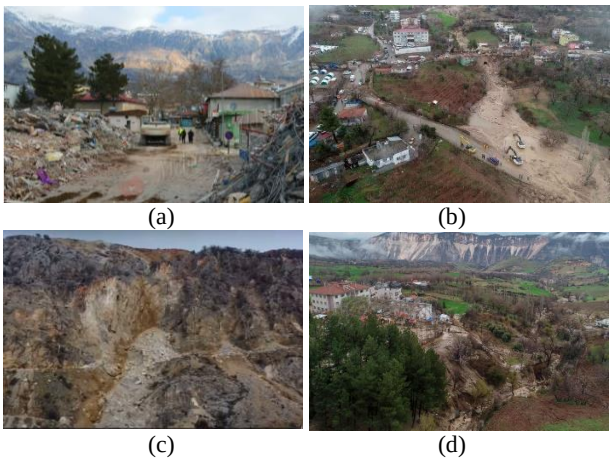

(a) (b) (c) (d)

Figure 2. Photos from Tut, Adiyaman: (a) (c) landslides triggered with the Kahramanmaras earthquakes occurred on 6 February 2023, (b) flooding occurred on 15 March 2023, and (d) landslides and flooding in Tut town (Gaziantep Time, TRT Haber, 2023).

2.2. Geological Characteristics and Landslide Inventory

The study area has a complex structure as it is located within the East Anatolian Fault Zone (EAFZ) with high seismicity. There are various units composed of igneous, metamorphic, and sedimentary rocks formed in the geological time period from the Precambrian to the present. There are twenty-seven lithological units in the study area as shown in Figure 3. The numbers are explained in Table A1 in Appendix. As can be seen in Figure 3 (see also Table A1 in Appendix), the most frequently observed lithological units in the study area are Neritic limestone (Eocene), non-graded terrigenous clastics (Pliocene Quaternary) and pelagic limestone, radiolarite, chert (Middle Triassic-Cretaceous).

The landslide inventory was delineated manually from two sources; (i) from the General Directorate of Mineral Research and Exploration (MTA) geosciences WebGIS portal, (ii) by comparing pre-and post-earthquake orthophotos presented by General Directorate of Mapping HGM Küre application (HGM, 2023; MTA, 2023). A total of 634 landslide polygon was used in

the study. The minumum and maximum landslide areas in the inventory are 0.0001 km^2 and 3.92 km^2, respectively. The landslide inventory is also shown on EUDEM v1.1 in Figure 1.

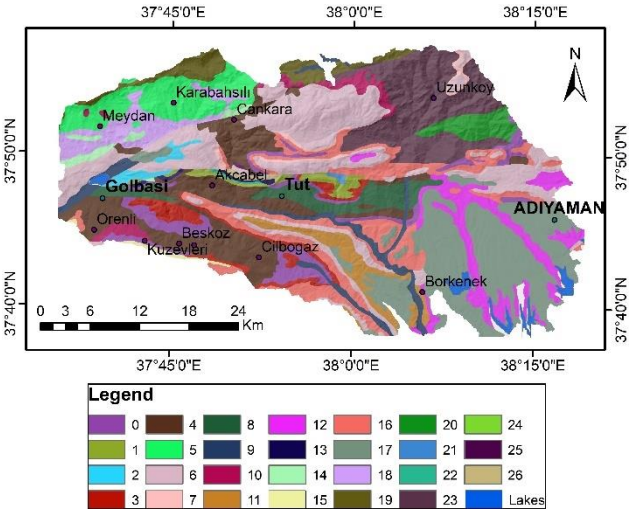

Figure 3. The lithological map of the study area.

2.3. Geospatial Datasets and Conditioning Factors

The conditioning factors used in the study can be categorized as *topographical* (altitude, slope, aspect, plan and profile curvature, stream power index - SPI, topographic wetness index - TWI, distance to drainage networks), *geological* (lithology, distance to faults) and *environmental* (land use land cover - LULC). The geospatial datasets, their characteristics and the data sources are presented Table 1.

Category-related factors	Format	Scale/ Resolution	Source
Topographical (altitude, slope, aspect, plan and profile curvature, SPI, TWI, distance to drainage network)	Grid	25 m	EU-DEM v1.1
Geological (Lithology, Faults)	Polygon Polyline	1:100,000 1:25,000	MTA
Environmental (LULC)	Grid	10 m	ESA WorldCover

Table 1. The conditioning factors and respective geospatial data sources used in the study.

The topographical factors were produced from EUDEM v1.1 with a grid size of 25 m. Lithology and faults data, which are geological factors, were digitized from geosciences WebGIS portal and geological maps published by MTA. The LULC data was obtained from ESA World Cover mapping (ESA WorldCover, 2021). The open source SAGA tool and the ArcGIS software from ESRI was used for this process.

2.4. Production of Univariate Susceptibility Maps

In the study, univariate maps were produced individually for landslide, flood and earthquake hazards. The RF algorithm proposed by Breiman (2001) has been frequently used in the literature for landslide susceptibility map production and is known to provide high accuracy for this purpose (e.g. Karakas et al., 2020, 2023). Before applying the model, Randomized search CV method was utilized for parameter optimization of the model. The optimum parameter values determined by Randomized Search CV of the RF algorithm used in the study to produce a landslide susceptibility map are shown in Table 2.

Model	Hyperparameter	Value
Random Forest	n_estimators	344
	criterion	'entropy'
	max_depth	20
	min_samples_split	2
	min_samples_leaf	2
	class_weight	'balanced'
	bootstrap	'false'

Table 2. Optimum parameter values obtained with RandomizedSearchCV

The pixels in the inventory polygons were used as landslide samples for the training. The non-landslide samples were selected randomly. As a result, a total of 118,668 landslide and 178,002 non-landslide pixels (a total of 2,670,030 pixels for all features) were utilized in the training process. The training and test samples were split using a ratio of 80/20. For model accuracy assessment, the area under the receiver operating characteristic (ROC) curve (AUC), precision, recall, overall accuracy, and F-1 score measures were used for validating with test samples.

The flood susceptibility map was produced by an expert-based method, the M-AHP (Nefeslioglu et al. 2013). This method was preferred due to the lack of flood inventory data in the study area. Expert subjectivity in pairwise factor comparisons in traditional AHP method is eliminated by the M-AHP. Thus, it is preferrable to use the M-AHP method. The Python programming environment was used to implement both the landslide and the flood susceptibility maps.

The seismic hazard map of the study area was generated using the inverse distance weighting (IDW) interpolation method based on Arias intensity values (Arias, 1970). The study area was classified relatively in terms of the effects of earthquakes using arias intensity. For this purpose, arias intensity records of the study area and surrounding forty-six accelerometer stations obtained from the AFAD earthquake database were used (AFAD TADAS, 2023).

2.5. Multi-hazard Susceptibility Assessment

The univariate susceptibility maps were combined with Mamdani FIS (Mamdani and Assilian, 1975) and the multi-hazard susceptibility map of the study area were obtained. The method is intuitive as experts define the rules as linguistic variables. The membership functions allow providing crisp inputs. The defuzzification step translates the outputs again to linguistic variables. The memberships functions defined here are presented in Figure A1 in Appendix. The rules can be found in Karakas et al. (2023).

3. RESULTS AND DISCUSSIONS

Here, the feature maps, the univariate hazard susceptibility maps, the multi-hazard susceptibility maps and the validation results are presented.

3.1. Conditioning Factors Results

The feature maps of the conditioning factors required for landslide and flood susceptibility production are given in Figure A2 in Appendix. While conditioning factors such as altitude, slope, aspect, plan and profile curvatures, SPI, TWI, lithology and distance to faults were utilized for landslide susceptibility mapping; altitude, slope, TWI, distance to drainage networks, lithology and LULC were employed for flood susceptibility mapping.

3.2. Univariate Susceptibility Map Results

In the present study, landslide susceptibility map was produced by the RF algorithm using nine conditioning factors. As can be seen in Table 3 and Figure 4, high accuracy could be obtained from the model. The AUC value from the model was 0.98. The corresponding overall accuracy of the model was 0.94, and F-1 score was 0.93 for landslide class.

Class	Precision	Recall	F-1 Score
Non-landslide	0.97	0.93	0.95
Landslide	0.91	0.96	0.93

Table 3. The statistical metrics of RF algorithm

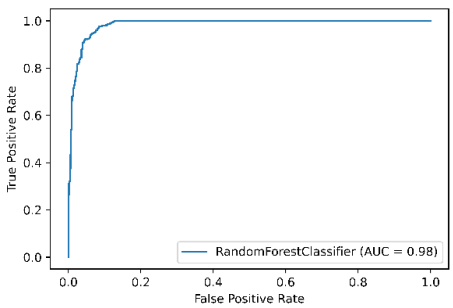

Figure 4. The AUC value obtained from the RF.

The univariate susceptibility maps are illustrated in Figure 5 (a-c). When evaluating the results for landslide susceptibility, it was observed that the probability of landslides is very high in the mountainous areas in the north of Tut town and in the south of Golbasi town. Visual similarities were detected between greater slopes (see Figure A2c in Appendix) and higher landslide susceptibility values (Figure 5a) in the study area. The flood susceptibility map indicates that areas located around Tut and Golbasi town and in the center of Adıyaman Province are highly susceptible. A preliminary assessment after the flood event occured in the region on 15 March 2023 indicated that the map accurately illustrate the flood-prone areas. When the seismic hazard map was analyzed, the study area generally showed high-intensity values. The values were even higher especially in the northern and southern parts.

3.3. Multi-hazard Susceptibility Map Result

The gradient multi-hazard susceptibility map obtained from the Mamdani FIS showed that the southern and nouthern parts of the study area were very high susceptibility levels (Figure 5d). The multi-hazard susceptibility result indicated that the highly prone areas were located in the Karabahsili, Cankara, Uzunkoy, Orenli, Beskoz, Kuzevleri, Cilbogaz and Borkenek settlements. In addition, the northern part of the Tut town and the southern part of the Golbasi town are among the multi-hazard susceptible areas. In the literature, the univariate susceptibility maps have usually been combined with overlay analysis. The use of Mamdani FIS in this study increased the usability of the final multi-hazard map. Because in this method, the multi-hazard map was produced by determining the rules for each hazard and the weights for each membership function.

In Figures 6 and 7, detailed representations of part of univariate susceptibility maps and multi-hazard susceptibility map are presented. Due to higher Arias intensity and landslide susceptibility values, these parts of the study area yielded very high susceptibility levels.

4. CONCLUSIONS AND FUTURE WORK

Based on the proposed multi-hazard assessment approach, involving supervised (random forest for landslide susceptibility) and expert-based (M-AHP for flood susceptibility and Mamdani FIS for multi-hazard susceptibility) methods, the multi-hazard susceptibility map of the study site was produced here. The Arias intensity values were used after the IDW processing for assessing the earthquake hazard. The proposed approach can contribute to studies such as site selection in areas prone to multiple natural hazards, sustainable land use planning and mitigation of future hazards. This issue is currently crucial for Türkiye as extensive construction projects have just been initiated after the Kahramanmaras earthquakes due to the immense need of new buildings as over 185,000 residential units were destructed (Adiyaman Valiligi, 2023).

As future work, risk assessments with vulnerable elements are also planned. Generalization capability and scalability of the proposed method will be investigated for different geographic regions and using various conditioning factors.

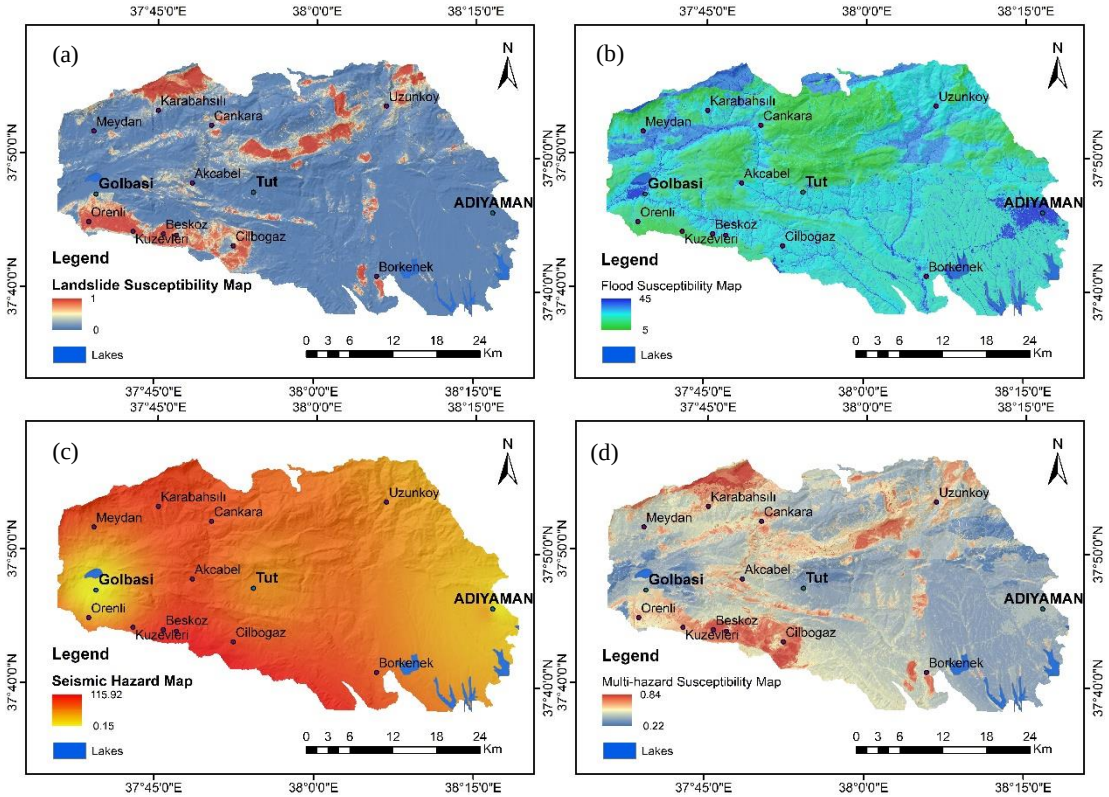

Figure 5. The univariate susceptibility results map: (a) landslide susceptibility, (b) flood susceptibility, (c) seismic hazard, and (d) multi-hazard susceptibility maps.

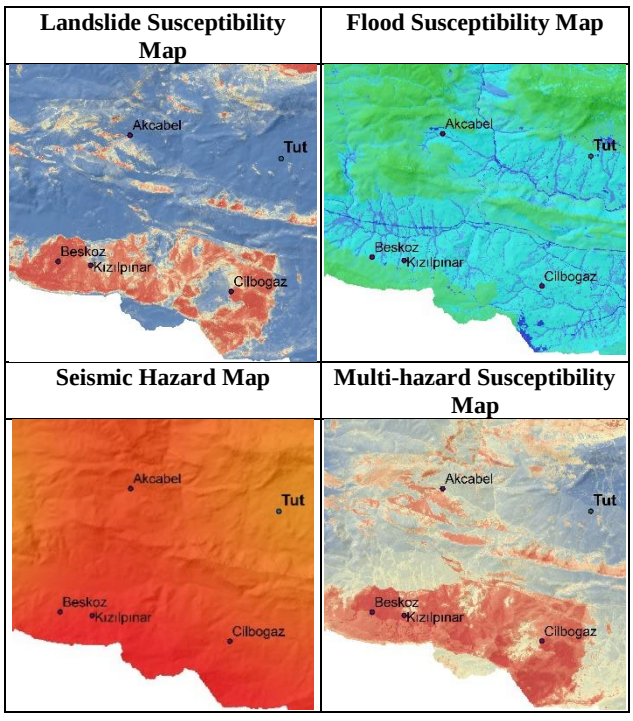

Figure 6. The univariate and multi-hazard susceptibility maps over Tut town of Golbasi, Adiyaman and surroundings.

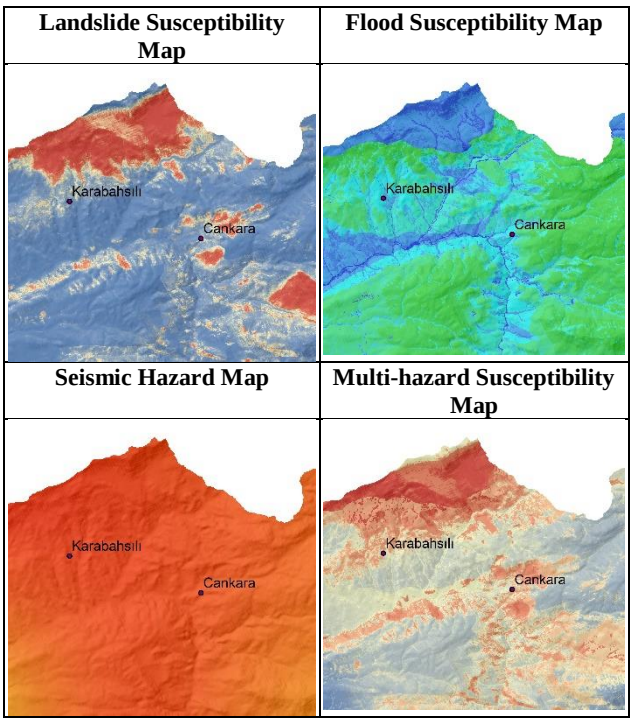

Figure 7. The univariate and multi-hazard susceptibility maps over Karabahsili and Cankara villages of Golbasi, Adiyaman.

ACKNOWLEDGEMENTS

This study is part of the PhD thesis research of Gizem Karakas. Authors gratefully acknowledge the support of Dr. Nazlı Tunar Ozcan, Sinem Cetinkaya and Veysel Emre Karakas for this study.

REFERENCES

Adiyaman Valiligi, 2023. URL: http://www.adiyaman.gov.tr/cumhurbaskanimiz-sn-erdogan-sehrinize-sahip-cikin-ata-yurdunuzu-asla-kalici-olarak-terk-etmeyin-merkezicerik (last accessed on 12 April 2023).

AFAD TADAS, Turkish Accelerometric Database and Analysis System), 2023. URL: https://tadas.afad.gov.tr/login (last accessed on 4 June 2023).

Arias, A. 1970. Measure of earthquake intensity. In Seismic design for nuclear power plants, ed. R.J. Hansen, 438–483. Cambridge: MIT Press.

Breiman, L., 2001. Random Forests. Machine Learning, 45, 5–32.

ESA-WorldCover V2. 2021. Worldwide land cover mapping: VITO NV.2021. URL:https://esa-worldcover.org/en. (last accessed on 4 June 2023).

HGM (General Directorate of Mapping), 2023. HGM Küre Application. URL: https://hgmkure.btk.gov.tr/ (last accessed on 10 April 2023).

Karakas, G., Can, R., Kocaman, S., Nefeslioglu, H.A., Gokceoglu. C., 2020. Landslide susceptibility mapping with random forest model for Ordu, Turkey. Int. Arch. Photogramm. Remote Sens. Spatial Inf. Sci., XLIII-B3-2020, 1229–1236, https://doi.org/10.5194/isprs-archives-XLIII-B3-2020-1229 2020.

Karakas, G., Kocaman, S., and Gokceoglu, C., 2023. A Hybrid Multi-Hazard Susceptibility Assessment Model for a Basin in Elazig Province, Türkiye. Int J Disaster Risk Sci. https://doi.org/10.1007/s13753-023-00477-y.

Mamdani, E.H., and Assilian, S., 1975. Experiment in linguistic synthesis with a fuzzy logic controller. International Journal of Man-Machine Studies 7(1): 1–13. https://doi.org/10.1016/S0020-7373(75)80002-2.

MTA (General Directorate of Mineral Research and Exploration), 2023. GeoScience Map Viewer. http://yerbilimleri.mta.gov.tr/ (last accessed on 10 April 2023).

Nefeslioglu, H.A., Sezer, E.A., Gokceoglu, C., and Ayas, Z., 2013. A modified analytical hierarchy process (M-AHP) approach for decision support systems in natural hazard assessments. Computers & Geosciences 59: 1–8. https://doi.org/10.1016/j.cageo.2013.05.010.

Pourghasemi, H.R., Kariminejad, N., Amiri, M. et al., 2020. Assessing and mapping multi-hazard risk susceptibility using a machine learning technique. Sci Rep 10 (3203). https://doi.org/10.1038/s41598-020-60191-3.

Rahmati, O., Yousefi, S., Kalantari, Z., Uuemaa, E., Teimurian, T., Keesstra, S., Pham, T.D., Tien Bui, D., 2019. Multi-Hazard Exposure Mapping Using Machine Learning Techniques: A Case Study from Iran. *Remote Sens, 11* (1943). https://doi.org/10.3390/rs11161943.

Tiryaki, M., and Karaca, O. 2018. Flood susceptibility mapping using GIS and multicriteria decision analysis: Saricay-Çanakkale (Turkey). Arabian Journal of Geosciences 11(14): Article:364. https://doi.org/10.1007/s12517-018-3675-3.

TRT Haber, 2023.
URL: https://www.youtube.com/watch?v=Y_aUUCpgqms (last accessed on 13 April 2023).

Yanar, T., Kocaman, S., and Gokceoglu, C., 2020. Use of Mamdani Fuzzy Algorithm for multi-hazard susceptibility assessment in a developing urban settlement (Mamak, Ankara, Turkey). ISPRS International Journal of Geo-Information 9(2): Article 114. https://doi.org/10.3390/ijgi9020114.

APPENDIX

ID	Lithological Unit	Area (km^2)
0	Clastics and carbonates (flysch)	72.33
1	Neritic limestone (Cretaceous)	18.01
2	Clastics and carbonates (Miocene)	12.58
3	Pelagic limestone	40.019
4	Pelagic limestone,radyolarite,chert,	177.56
5	Undifferentiated basic and ultrabasic rocks	84.90
6	Neritic limestone (Eocene)	238.79
7	Terrigenous clastics (Eocene)	11.86
8	Pelagic limestone, clastics, radiolarite	53.60
9	Undifferentiated	48.25
10	Alluival fan, debris, moraine	25.81
11	Neritic limestone (Miocene)	38.89
12	Terrigenous clastics (Miocene)	86.95
13	Carbonates and clastics (Cretaceous)	4.69
14	Carbonates and clastics (Middle Eocene Lower Miocene)	13.76
15	Neritic limestone (Paleocene)	5.43
16	Carbonates and clastics (Upper Cretaceous-Eocene)	136.29
17	Non-graded terrigenous clastics	234.85
18	Volcanites and sedimentary rocks (Upper Eocene - Lower Oligocene)	51.64
19	Marble, schist in places	42.02
20	Ophiolitic melange	28.23
21	Clastics (Precambrian)	1.74
22	Clastics (Ordovician)	1.88
23	Volcanites and sedimentary rocks (Middle Triassic Cretaceous)	154.19
24	Peridotite	0.01
25	Basalt	0.67
26	Clastics (Precambrian)	4.32

Table A1. Lithological units with the area in the study area

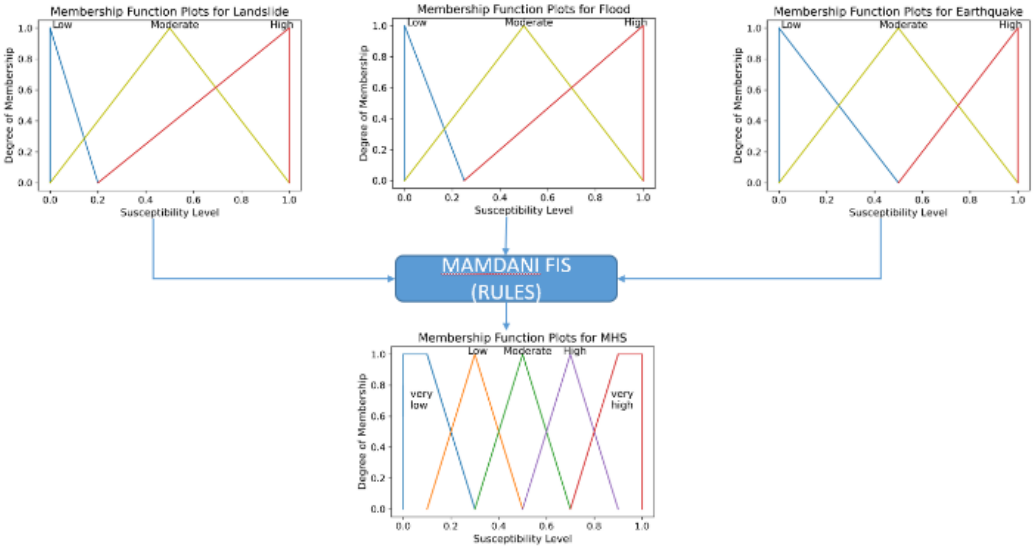

Figure A1. Membership functions defined for Mamdani FIS.

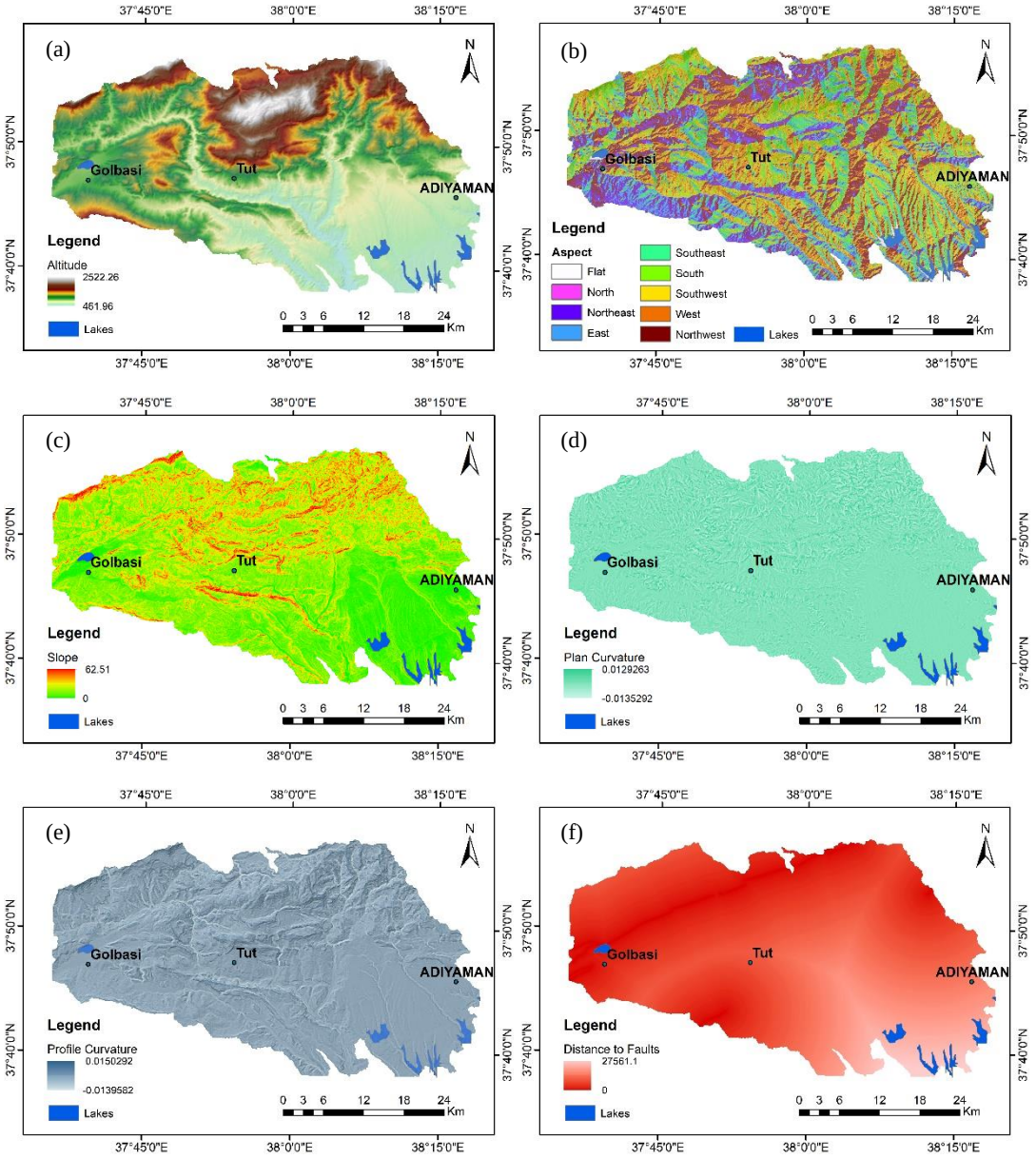

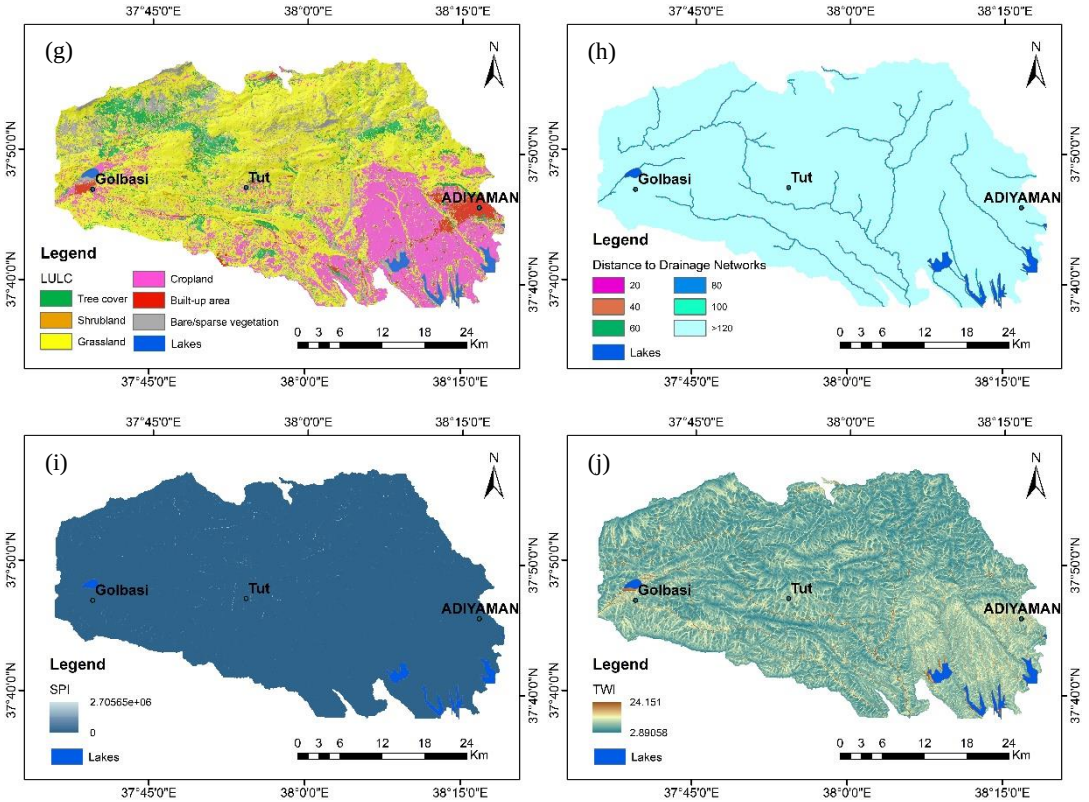

Figure A2. Conditioning factors used in the study for landslide and flood susceptibility assessment: (a) altitude, (b) aspect, (c) slope, (d) plan curvature, (e) profile curvature, (f) distance to faults, (g) LULC, (h) distance to drainage networks, (i) SPI, (j) TWI